

# Adaptive Control of Ultrasonic Motors Using the Maximum Power Point Tracking Method

Markus Flueckiger, José M. Fernandez, and Yves Perriard, *Senior Member IEEE*  
 Ecole Polytechnique Fédérale de Lausanne (EPFL), Institut de Microtechnique (IMT)  
 Laboratoire d'Actionneurs Intégrés (LAI), Station 11, CH - 1015 Lausanne, Switzerland  
 Email : markus.flueckiger@epfl.ch, jose.fernandez@epfl.ch, yves.perriard@epfl.ch

**Abstract**—The properties of ultrasonic piezoelectric motors depend on applied load and temperature. The output behaviour is characterized by the nonlinearity of the power transmission at the friction interface between stator and rotor. Because of these inherently nonlinear characteristics, a resonant frequency tracking control is imperative for some particular applications where direct speed or position sensing is not applicable and harsh environment conditions with large thermal gradients and important load variations subsist. We suggest a maximum power point tracking (MPPT) approach, which is well known from contactless energy transmission systems. The MPPT controller was compared to a phase-locked loop controller for ultrasonic motors known from literature. The resonant frequency can be tracked over a far wider working range compared to the phase locking range. Also, the MPPT control circuit is very easy to tune and no sophisticated loop gain design is needed. The analog version of the MPPT controller was built and tested with linear and rotary ultrasonic motors.

## I. INTRODUCTION

Piezoelectric actuators are nowadays established in industrial applications, where their well known advantages make them superior to electromagnetic micro motors. Nevertheless, certain reservations remain, particularly with respect to control strategy and the corresponding electronic circuitry.

It is best practice to consider the motor with the electronic circuitry as one single system that should present an optimal overall behaviour. In this way, it is possible to design a motor that is driveable over a large working range, including important temperature variations and load cycles. However, there are limits to this design approach.

For an ultrasonic motor that is driven by a resonant converter, the electric resonant frequency of the drive circuit must match mechanical resonance of the piezoelectric actuator. In this case and with constant load and ambient conditions, power transmission to the piezoelectric element is maximal at the resonant frequency of the vibrator. However, resonant frequency tracking is necessary when piezoelectric motors are used in harsh environment with large thermal gradients and important load variations, that modify the resonant frequency.

In order to develop an adaptive controller we need to understand the factors that introduce the variations of the resonant frequency and the concepts used for resonance matching.

## II. RESONANCE MATCHING

The Van-Dyke model of a piezoelectric resonator [1] models the vibrator resonating at the frequency  $\omega_m$  with an equiva-

lent electrical impedance. The motional capacitance  $C_m$  and motional inductance  $L_m$  represent the rigidity and the inertia of the vibrator, respectively. The mechanical losses of the vibrator are modelled with  $R_m$ . A block diagram of the power supply representing the piezoelectric element with this electric equivalent circuit is shown in Figure 1.

The sharpness of the resonance is indicated by the electrical quality factor  $Q$ :

$$Q = \frac{1}{\omega_m C_m R_m} \quad (1)$$

For optimal power transfer, the motional admittance  $Y_m$  of the excited system must equal the electric admittance  $Y$ . This translates to matching the electrical resonant frequency to the mechanical resonant frequency of the ultrasonic motor.

The motional admittance in terms of the quality factor  $Q$  is:

$$Y_m = \frac{1}{R_m(1 + jQ(\frac{\omega}{\omega_m} - \frac{\omega_m}{\omega}))} \quad (2)$$

where the dissonance between the mechanical resonance and the excitation is expressed with  $\frac{\omega}{\omega_m} - \frac{\omega_m}{\omega}$ .

Using this expression, the total admittance seen by the supply when considering the static capacitance of the piezoelectric vibrator  $C_0$  can be approximated around resonance as:

$$Y = Y_0 + Y_m = j\omega_m C_0 + \frac{1}{R_m(1 + jQ(\frac{\omega}{\omega_m} - \frac{\omega_m}{\omega}))} \quad (3)$$

The admittance magnitude maximum at the mechanical resonant frequency is slightly shifted with respect to the first zero crossing of admittance phase at serial resonance  $\omega_s$ . Similarly, antiresonance, where the admittance magnitude is

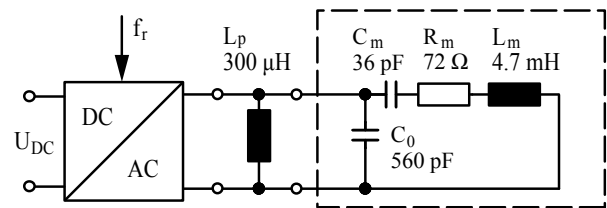


Figure 1. Supply diagram with electric equivalent circuit for the piezoelectric element

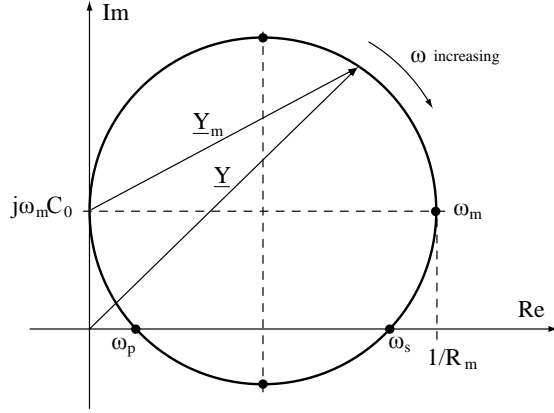


Figure 2. Admittance locus of the piezoelectric element

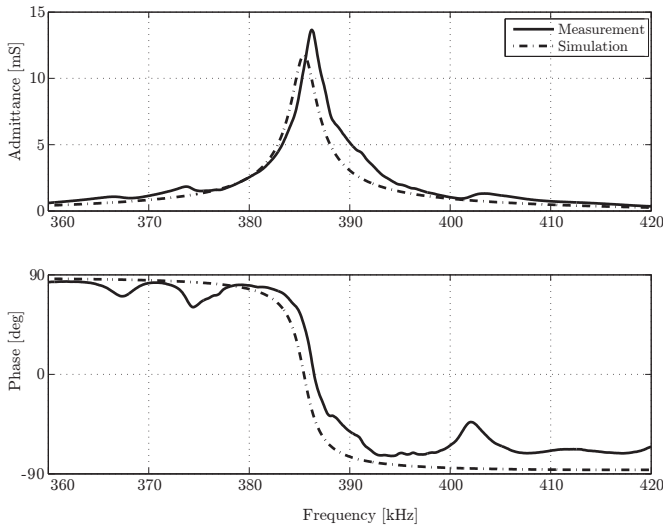


Figure 3. Impedance characteristics of the piezoelectric element

minimal, does not coincide with the second zero crossing at parallel resonance  $\omega_p$ . This situation is well illustrated by the off-centred unity circle in the admittance locus in Figure 2.

For a given frequency, which is in our case the mechanical resonant frequency where vibration amplitude is maximal, this effect of the static capacitor can be compensated by an inductor  $L_p$  in parallel to  $C_0$ :

$$L_p = \frac{1}{\omega_m^2 C_0} \quad (4)$$

This inductor consumes the reactive component of the current and hence the corresponding unity circle in the admittance locus is centered at the real axis. The mechanical resonant frequency  $f_r$  and the series resonance  $f_s$  are thus equal in the ideal case of perfect matching. The parallel resonance  $f_p$  disappears [2].

For model verification, the equivalent model parameters were measured. The corresponding Bode plot (Figure 3), compares the PSpice simulation of the electric equivalent

circuit and the results of impedance analysis with an Agilent 4294A precision impedance analyzer.

### III. MAXIMUM POWER POINT TRACKING

Adjusting the optimal working point by the means of maximum power point tracking is a widely known practice which is used mainly in solar power systems and wireless energy transfer. We evaluate if the principle applies to the case of driving a piezoelectric motor, because by definition, maximal power is transmitted to the piezoelectric element at resonance where impedance is minimal. Basically, power point tracking may be implemented either in a continuous way for analog control and with a discrete approach for digital control [3]. The electric resonant frequency of the drive circuit must match mechanical resonance of the piezoelectric actuator. Then, for given load and ambient conditions, the maximum transmissible power corresponds to the optimal working frequency. The instantaneous power is composed of the reactive power and the active power  $p$  which is proportional to the power transmitted to the actuator. It is measured indirectly by multiplication of phase current and line voltage (Figure 4).

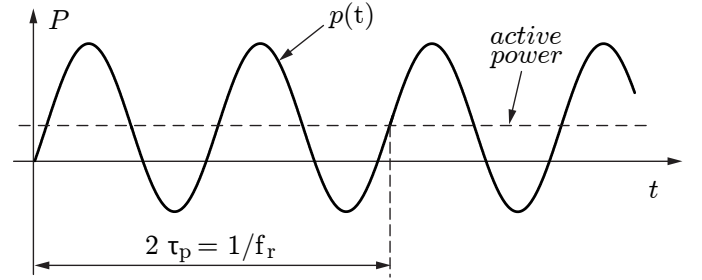


Figure 4. The measured value is the variation in active power  $\Delta P_d$ ; the period of instantaneous power  $\tau_p$  is twice the period of the excitation  $1/f_r$  by definition.

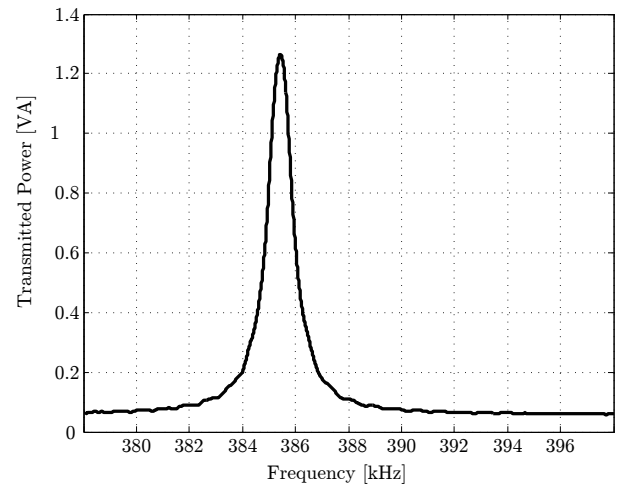


Figure 5. Power maximum of a piezoelectric actuator driven by a resonant converter and resonant frequency at 385.5 kHz.

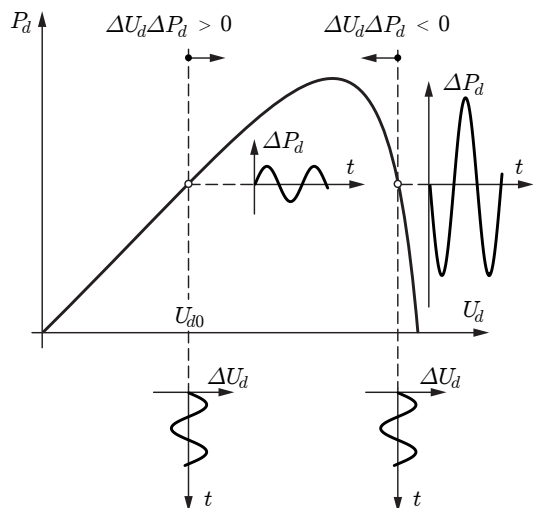


Figure 6. Continuous maximum power point tracking

Instead of applying a constant frequency  $f_0$  to the power device, a variation  $\Delta f$  is superposed on the constant value. This variation generates a variation of power  $\Delta p$ . If the signals  $\Delta f$  and  $\Delta p$  are in phase, the system is on the positive slope of the power curve. Hence the frequency value  $f_0$  must be increased. On the negative slope, they are out of phase and  $f_0$  must be decreased. As the power curve presents a global maximum at the optimal frequency, the system is stable. For a hollow cylinder ultrasonic motor driven by a resonant converter and resonant frequency at  $385.5 \text{ kHz}$ , the power transmission characteristics are shown in Figure 5.

Figure 6 illustrates the continuous maximum power point tracking principle, whereas only the region around the power maximum is shown. The working frequency is generated by a voltage controlled oscillator (VCO). A periodic variation of  $\Delta U_d$  is added to the constant VCO control voltage  $U_{d0}$ . The frequency of this variation is around  $1 \text{ kHz}$  (well below the working frequency at standard conditions of  $385.5 \text{ kHz}$  and significantly higher than  $50 \text{ Hz}$ ), introducing a variation  $\Delta P_d$  to the mean power  $P_d$ . At a frequency below the optimal working point, the product of  $\Delta U_d$  and  $\Delta P_d$  is positive ( $\Delta U_d \Delta P_d > 0$ ). This is easily exploited to increase  $U_{d0}$  in order to reach the optimal working point. Contrarily, at a frequency above the optimal working point,  $\Delta U_d \Delta P_d < 0$ , which allows for reducing  $U_{d0}$  by the means of a control circuit. Finally, at the optimal working point,  $\Delta U_d \Delta P_d \cong 0$  and  $U_{d0}$  is maintained. Hence this strategy is very appropriate for analog control [4].

Figure 7 shows a signal flow diagram of the maximum power point tracking electronic circuitry as it has been realised. The working frequency, which equals at steady state the resonant frequency  $\omega_m$ , is obtained by a VCO. The VCO is controlled by the filtered output of the XOR gate. This DC voltage is proportional to the phase difference between the perturbation voltage  $\Delta U_d$  and the resulting variation of active

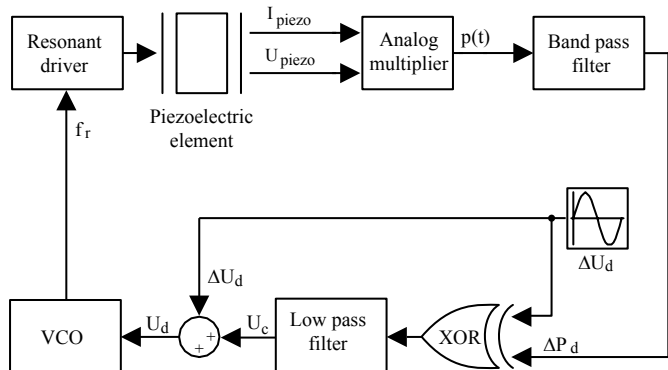


Figure 7. Signal flow diagram of the maximum power point tracking electronic circuitry

power  $\Delta P_d$ . This power variation is observed by analog multiplication of phase current and line voltage. An appropriate band pass filter allows for distinguishing rigorously between the oscillations at working frequency and the oscillations associated with the maximum power point observation.

#### IV. RESULTS

The MPPT controller was compared to a phase-locked loop controller for ultrasonic motors known from literature, by the means of PSpice simulations for the analog case, and an implementation on microcontroller for the discrete case. In both cases, the resonant frequency can be tracked over a far wider working range compared to the phase locking range. Also, the MPPT control circuit is very easy to tune and no sophisticated loop gain design is needed. The analog version of the MPPT controller was built and tested on linear and rotary ultrasonic motors. The closed loop transient response is shown in Figure 8. The VCO control voltage reaches the level corresponding to the resonant frequency at standard conditions after a rise time of  $9 \text{ ms}$  with an overshoot of  $7.5\%$ . The controller settles after  $27.5 \text{ ms}$  in a band of  $\pm 4\%$ , which is

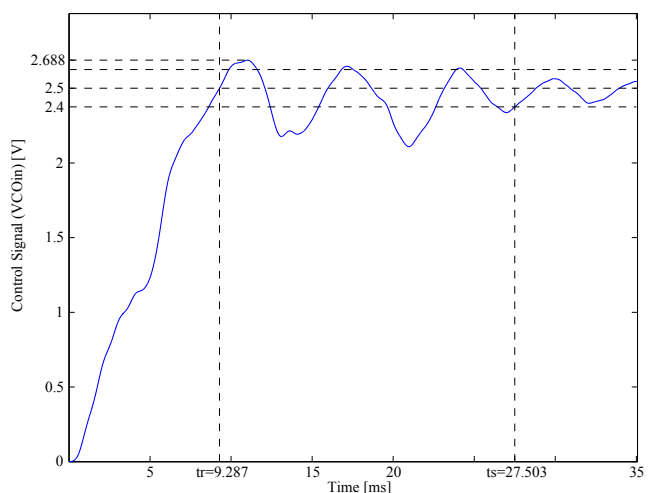


Figure 8. Transient response of the maximum power point tracking controller.

acceptable for motor operation. However, the response time is slow compared to a PLL based adaptive controller, which have settling times of a few milliseconds.

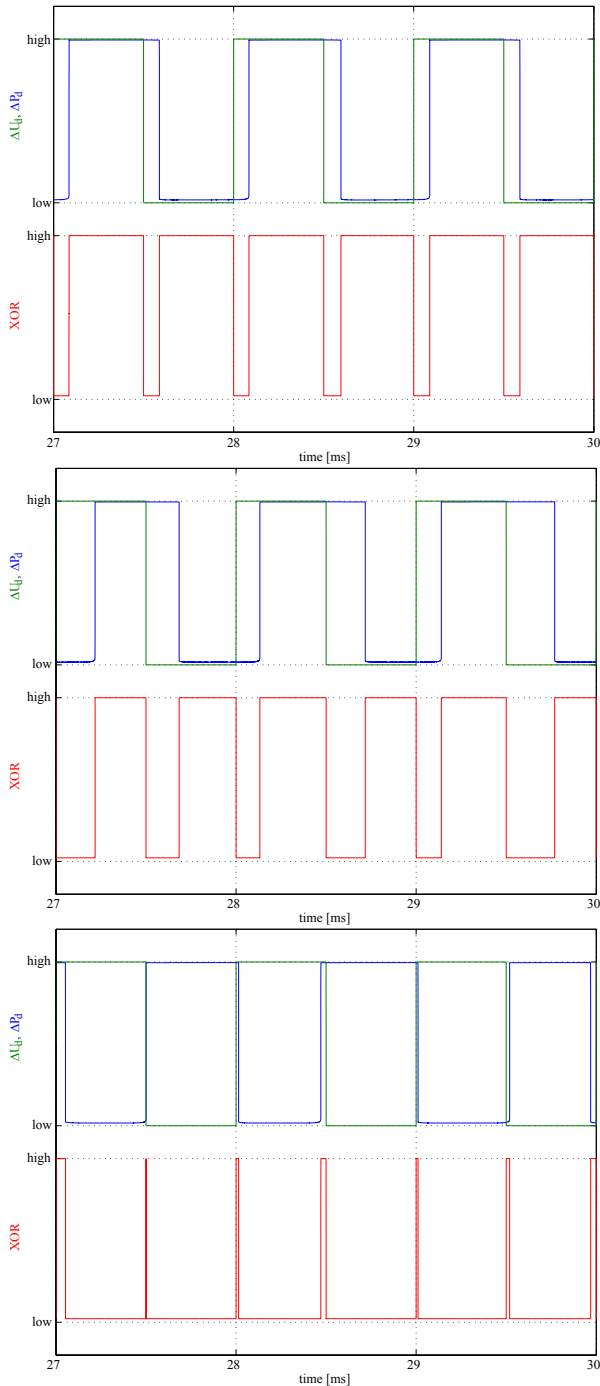


Figure 9. Open loop characteristics of the maximum power point tracking controller. **Top:** Perturbing signal and observed power variation with the resulting XOR output signal at  $1/10$  of the resonant frequency. Signals are in phase and the XOR output is high. **Center:** Perturbing signal and observed power variation with the resulting XOR output signal at the resonant frequency. Power leads by  $\pi/2$ , the XOR output is a half duty cycle signal. **Bottom:** Perturbing signal and observed power variation with the resulting XOR output signal at 2 times the resonant frequency. Phase shift is  $\pi$ , the XOR output is low.

Measurements of the open loop characteristics (Figure 9) show that the power maximum is clearly detectable and the effects of the perturbation on drive characteristics are neglectable.

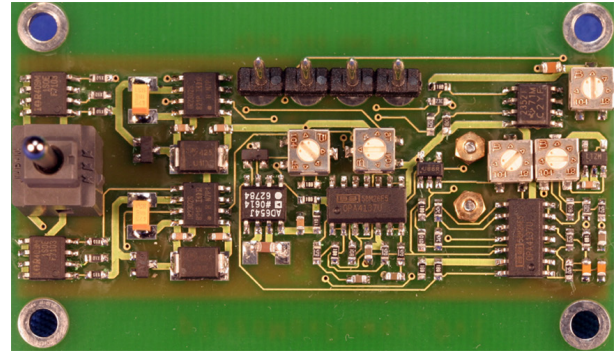


Figure 10. Prototype printed circuit board implementing a MPPT controller

The analog controller was implemented on a printed circuit board (Figure 10).

## V. CONCLUSION

A new adaptive controller for ultrasonic motors has been developed. No motor model is needed and the only parameter to be determined is the impedance of the motor for initial resonance matching. Results showed that performance of the MPPT controller is comparable to state of the art phase-locked control loops, but it is able to track the optimal frequency over a much wider range without any stability concerns. Offsets of the electronics are automatically compensated. However, the variable frequency component applied for indirect measurement purposes may influence the motor behaviour. Further research on this subject is necessary to find an optimised configuration.

## ACKNOWLEDGMENT

The authors would like to thank Philippe Vosseler and his team at ACI-EPFL for important advice on PCB routing as well as Stéphane Burri and Paolo Germano at LAI-EPFL for their assistance with prototyping.

## REFERENCES

- [1] A. Arnau, Y. Jimenez, and T. Sogorb, "An extended butterworth van dyke model for quartz crystal microbalance applications in viscoelastic fluid media," *Ultrasonics, Ferroelectrics and Frequency Control, IEEE Transactions on*, vol. 48, no. 5, pp. 1367–1382, 2001.
- [2] C. Péclat, *Conception et réalisation d'un micromoteur piézoélectrique*. PhD thesis, Département d'électricité, Ecole Polytechnique Fédérale de Lausanne, Lausanne, Switzerland, 1995.
- [3] H. Bühler, *Convertisseurs Statiques*. Presses Polytechniques et Universitaires Romandes, 1991.
- [4] P. Germano and M. Jufer, "Contactless power transmission : Frequency tuning by a maximum power tracking method," in *EPE'97 Trondheim*, vol. 4, pp. 693–697, 1997.